A K-Band UWB Low-Noise CMOS Mixer With Bleeding Path G_m-Boosting Technique

Sunwoo Kong, *Student Member, IEEE*, Choul-Young Kim, *Associate Member, IEEE*, and Songcheol Hong, *Member, IEEE*

***Abstract*—A low-noise ultrawideband CMOS mixer circuit for the down conversion of a K-band signal is presented. A bleeding path g_m-boosting technique is proposed, which reduces the effect of noise sources of the proposed mixer. The measurement results show that the minimum noise figure is 3.61 dB at 24 GHz when consuming 2.6 mW at a 1.5-V supply voltage. The results also show a conversion gain of 9.15 dB, a $P_{1\,\mathrm{dB}}$ of -13 dBm, and an isolation of a local oscillator port to a radio frequency port of -40 dB. The circuit was fabricated using 0.13-μm CMOS technology with a chip area of 0.68×1.07 mm^2.**

***Index Terms*—CMOS, current bleeding, g_m-boosting technique, low noise, mixers.**

I. Introduction

RADAR is a distance-measuring sensor system, and it is being more widely applied as radar systems are becoming smaller with integrated circuit technology. Automotive systems, medical imaging systems, robot vision systems, security and safety systems, tank level meters, human–device interaction systems, and so on are rapidly being developed, which incorporate radar technology. These radar systems can be implemented with low cost due to CMOS technology, which makes it possible for radar systems to be used in more applications.

Ultrawideband (UWB) radar measures a distance by transmitting and receiving short pulses that have a very wide spectrum. The shorter the pulsewidth becomes, the better the range resolution of the radar system is, and this means that the pulse signal has a wider bandwidth. An unlicensed 7-GHz-wide spectrum of 22–29 GHz with strict emission restrictions has been allocated by the Federal Communications Commission [1]. A UWB radar system should have a wide bandwidth to obtain high-range resolution using a pulse signal with a very short pulsewidth. Radar systems can lead to collision with other wireless systems because they use very wideband signals. Therefore, to prevent this problem, the transmitted power is restricted to very low levels. Integration of pulses is used to improve signal-to-noise ratio (SNR) with this low transmitted power. However, integration of many pulses takes long sweep time. This means that tracking targets are not processed in real time. UWB radar receivers should have very low noise figure to get an appropriate SNR at the receiver output with integration of fewer pulses or without integration. In a typical low-noise amplifier (LNA) and mixer chain, the LNA should have a high enough gain to suppress the noise of the mixer because mixers often produce a large amount of noise [2]. Moreover, the LNA should have a low noise figure and a wide bandwidth, simultaneously. An LNA operating at high frequency, such as the K-band, is used to have a high-Q load to obtain a high gain, but it brings a narrow bandwidth. Other gain-enhancing methods, such as improving transconductance and using multiple stages, can lead to problems of high power consumption and increased parasitic capacitance. A low-noise mixer makes relaxed requirements of an LNA, and furthermore, there can be no need for an LNA. Recently, radar systems with multiple transceivers for 2-D location have become important. Multiple transceivers enable better cross-range resolution because they make the larger antenna aperture [3]. Low power consumption of a transceiver becomes increasingly important due to the need for multiple transceivers.

This brief presents a low-noise mixer that has a wide bandwidth and low power consumption with the proposed bleeding path g_m-boosting technique. Section II describes the proposed bleeding path, which boosts the total transconductance of the mixer. In Section III, the noise analysis is given. Section IV presents the implementation and experimental results.

II. Proposed Low-Noise Mixer With Bleeding Path G_m-Boosting Technique

A conventional single-balanced mixer is made up of a radio frequency (RF) input transconductance stage, local oscillator (LO) switches, and output loads. An RF input signal is converted to a current signal by the transconductance stage, and it is translated to intermediate frequency (IF) by the LO switches.

Fig. 1 presents the proposed mixer. The mixer uses a common-gate input stage for wideband input matching. However, it is difficult to achieve a low noise figure because g_m, which is the transconductance of an input transistor, determines the input impedance of the common-gate structure. This means that $1/g_m$ should be the same as 50 Ω. A g_m-boosting technique must be applied to improve both the noise figure and the input matching [4]. If an inverting amplifier is connected between the source and the gate, an effective voltage, driving an input

Manuscript received August 23, 2012; accepted December 19, 2012. Date of publication March 7, 2013; date of current version March 14, 2013. This work was supported by the National Research Foundation of Korea grant funded by the Korea Government (Ministry of Education, Science and Technology) (No. 2009-0080805). This brief was recommended by Associate Editor T. Tong.

S. Kong and S. Hong are with the School of Electrical Engineering and Computer Science, Department of Electrical Engineering and Computer Science, Korea Advanced Institute of Science and Technology, Daejeon 305-701, Korea (e-mail: throckmorton@kaist.ac.kr; schong@ee.kaist.ac.kr).

C.-Y. Kim is with the Department of Electronics Engineering, Chungnam National University, Daejeon 305-764, Korea (e-mail: cykim@cnu.ac.kr).

Digital Object Identifier 10.1109/TCSII.2013.2240792

1549-7747/$31.00 © 2013 IEEE

Authorized licensed use limited to: Southern University of Science and Technology. Downloaded on May 28,2024 at 04:56:57 UTC from IEEE Xplore. Restrictions apply.

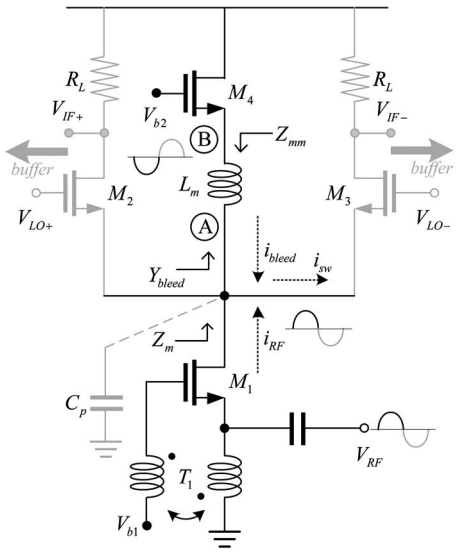

Fig. 1. Proposed bleeding path g_m-boosting technique.

transistor, will be increased. This brings an increased effective g_m without an increase in the bias current. Accordingly, the improved noise factor at the matched input impedance is given by

$$F_{CG,\text{gm-boosting}} = 1 + \frac{\gamma}{\alpha}\frac{1}{(1+A)^2 g_m R_s} = 1 + \frac{\gamma}{\alpha(1+A)}\bigg|_{(1+A)g_m R_s = 1} \quad (1)$$

where α and γ are empirical process- and bias-dependent parameters, and A is the gain of the inverting amplification. Here, R_s, i.e., a source impedance, is equal to $1/(1+A)g_m$ at the matched input impedance, and there remains only $(1+A)$ in the denominator. Thus, the noise figure can be improved by an increase in the value of A. The inverting amplifier is replaced by a passive low-noise transformer. This is a good alternative to the inverting amplifier. The value of A is defined by k, i.e., the coupling coefficient of the transformer T_1, and n, i.e., the turns ratio of T_1. A is equal to $n \times k$; therefore, the boosted transconductance is $(1+nk)g_{m1}$, where g_{m1} is the transconductance of M_1.

A current bleeding technique is used to make enough voltage head room at the drain of the switching stage without reducing the current in the transconductance stage and decreasing the value of the load resistor [5]. The current is injected from an nMOS bleeding path rather than the switching pair, maintaining the total current flowing through the transconductance stage. It is also possible to obtain a high conversion gain by using a larger load resistor with a finite supply voltage. However, there are two major problems associated with the current bleeding technique. The first problem is a leakage current flowing through parasitic capacitance C_p because of the increased impedance seen at the source of the switches. The other problem is additional noise from the current bleeding circuit itself. In this brief, the proposed bleeding path g_m-boosting technique resolves all these problems and lowers the noise of the mixer.

The basic idea is to boost the transconductance of the mixer without additional power consumption using the current bleeding circuit, which consists of the nMOS and the inductor. In the equation below, Y_{bleed} is expressed with M_4, which is the nMOS of bleeding path, and L_m, which is the inductor of bleeding path, i.e.,

$$Y_{\text{bleed}} = (g_{m4} + j\omega C_{gs4}) \| \frac{1}{j\omega L_m} = \frac{g_{m4} - j\left(\omega^3 L_m C_{gs4}^2 + \omega L_m g_{m4} - \omega C_{gs4}\right)}{(1-\omega^2 L_m C_{gs4})^2 + (\omega L_m g_{m4})^2}. \quad (2)$$

The parasitic capacitance seen at the drain of M_1, i.e., C_p, is cancelled out by making the imaginary part of Y_{bleed} have a negative value. Inductor L_m plays a major role such as [6]. From (2), the imaginary value of Y_{bleed} is heavily dependent on L_m. The transconductance of M_4, i.e., g_{m4}, and C_{gs4}, i.e., the gate–source capacitance of M_4, do not have a strong influence on it. Therefore, the value of L_m is determined to cancel out C_p; C_p is effectively cancelled out when $L_m = 1.5$ nH.

The connection between nodes A and B is shown below, i.e.,

$$v_B = -\frac{(\omega^2 L_m C_{gs4} - 1) + j\omega L_m g_{m4}}{(1-\omega^2 L_m C_{gs4})^2 + (\omega L_m g_{m4})^2} \cdot v_A = -u \cdot v_A. \quad (3)$$

According to (3), v_B, i.e., the voltage of node B, is made to have the opposite direction of v_A, i.e, the voltage of node A, by setting $\omega^2 L_m C_{gs4} > 1$. The requirements are met by selecting the proper size of M_4 because L_m is already fixed. It is sufficient to satisfy conditions with $W_4 = 150$ μm when $L_m = 1.5$ nH.

If v_B and v_A have opposite signs with the preceding condition, v_B will be negative when v_{RF} is positive, and vice versa. Consequently, the effective transconductance is boosted because i_{bleed} is also increased with the increase in i_{RF}. The total RF current with increased current from transformer T_1 is expressed in (4), and the increased current from the bleeding path is expressed in (5), i.e.,

$$i_{\text{RF}} = (1+nk) g_{m1} v_{\text{RF}} \quad (4)$$

$$i_{\text{bleed}} = g_{m4}(0 - v_B) = g_{m4} u \cdot v_A = g_{m4} u \cdot Z_m (1+nk) g_{m1} v_{\text{RF}}. \quad (5)$$

Here, Z_m is the impedance seen at the drain of M_1.

Fig. 2 shows the equivalent small-signal circuit model of the proposed mixer. Equation (2) explains that R_{bleed} is the reciprocal of the real value of Y_{bleed} and $\omega \cdot L_{\text{bleed}}$ is the reciprocal of the imaginary value of Y_{bleed}. Here, C_p is canceled out by L_{bleed} to remove the leakage current flowing through C_p. M_1 with boosting transformer T_1 leads to i_{RF}, and i_{RF} is divided and flows to R_{bleed} and R_{sw}. Note that R_{bleed} should be large enough to keep the bleeding path leakage current very low. Because L_m cannot be controlled for C_p cancelation, R_{bleed} is increased by enlarging the size of M_4. The increased size of M_4 can affect a bleeding path boosting factor; thus, it cannot be chosen yet. This is described later here. For example, R_{bleed} is equal to about 3.2 kΩ when $W_4 = 150$ μm and $L_m = 1.5$ nH. The bleeding path leads to i_{bleed}, and i_{bleed} is divided and

Authorized licensed use limited to: Southern University of Science and Technology. Downloaded on May 28,2024 at 04:56:57 UTC from IEEE Xplore. Restrictions apply.

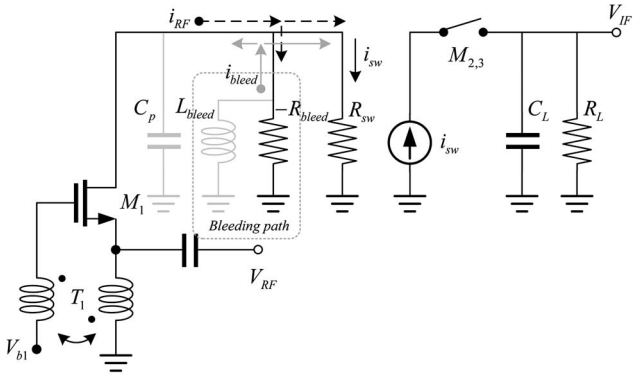

Fig. 2. Equivalent small-signal circuit model.

flows through M_1 and $R_{\rm sw}$, but the leakage current that flows to M_1 is very low because of the large output resistance of M_1. Therefore, $i_{\rm sw}$ is approximately equal to $i_{\rm RF} + i_{\rm bleed}$. As a result, the effective transconductance is enhanced as much as $(1 + g_{m4}u \cdot Z_m)$ in (6), i.e.,

$$g_{m,\text{effective}} = (1 + g_{m4}u \cdot Z_m)(1 + nk)g_{m1}. \tag{6}$$

The bleeding path boosting factor, i.e., $g_{m4}u \cdot Z_m$, must be increased to get the boosted transconductance from the bleeding path. When $\omega^2 L_m C_{gs4} \gg 1$, $g_{m4}u$ is expressed as

$$g_{m4}u = \frac{g_{m4}}{L_m} \frac{\omega^2 C_{gs4} + j\omega g_{m4}}{(\omega^2 C_{gs4})^2 + (\omega g_{m4})^2}. \tag{7}$$

Because L_m is already chosen to cancel out C_p, C_{gs4} and g_{m4} are controlled to enlarge $g_{m4}u$. How much v_B is contrary to v_A is shown by factor u. With the optimum C_{gs4} and g_{m4} ratio, the maximum $g_{m4}u$ is obtained. Increasing the size of M_4 is beneficial to meet the requirement for $\omega^2 L_m C_{gs4} \gg 1$ and to obtain a sufficient $R_{\rm bleed}$ to block leakage current. Above all things, $g_{m4}u$ is increased as the size of M_4 is increased. However, it becomes insignificant as it increases above a certain value because the effect of degeneration inductor L_m is enlarged. The size of M_4 is selected to get the optimum C_{gs4} and g_{m4} ratio when it is above the certain value.

The boosting factor $g_{m4}u \cdot Z_m$ is also controlled by the variation of Z_m due to the limit of increasing $g_{m4}u$. Equation (8) shows Z_m, i.e.,

$$Z_m = r_{o1} \left\| \frac{1}{g_{m2,3}} \right\| R_{\rm bleed}. \tag{8}$$

The Z_m value is approximately equal to $1/g_{m2,3}$, which is the resistance seen at the source of switch $M_{2,3}$ because r_{o1} and $R_{\rm bleed}$ are large enough. The transconductance of $M_{2,3}$ should be minimized to enlarge Z_m. This means that the bias current of switch $M_{2,3}$ is reduced and the bias current of bleeding path M_4 is increased to keep the transconductance of M_1 constant. The Z_m value cannot be continuously increased by reducing the switch current, as this is also limited. Reducing the switch current makes $i_{\rm RF}$ and $i_{\rm bleed}$ leak into the bleeding path and M_1 because it leads to large $1/g_{m2,3}$, which is comparable with r_{o1} and $R_{\rm bleed}$, and this reduces the effective transconductance. Therefore, $1/g_{m2,3}$ should be controlled to achieve large enough Z_m and insignificantly small leakage current simultaneously. The boosting value of the bleeding path, i.e., $1 + g_{m4}u \cdot Z_m$, is approximately equal to 2.2 with $W_4 = 150\ \mu$m and $L_m = 1.5$ nH at 24 GHz.

III. Noise Analysis

The proposed bleeding path with the g_m-boosting technique suppresses noise since it improves transconductance without an additional current, as compared with the conventional pMOS bleeding path. There are two types of mixer noise, namely, high-frequency noise and low-frequency noise [7]. The IF signal of UWB radar sensors is wideband. However, only the relatively high-frequency part of the IF signal is processed, and the low-frequency part is filtered out because the low-frequency signal near DC is seriously affected by the low-frequency noise, such as $1/f$ noise. Therefore, only the high-frequency noise in the mixer is taken into account. The output noise currents of the proposed low-noise mixer when C_p is cancelled out by the bleeding path and the LO signal is a square wave are shown below. As described earlier, most of noise currents from M_1 and M_4 are transferred to switch $M_{2,3}$ like the bleeding path g_m-boosting mechanism. The output noise currents from the contribution of M_1, M_4, $M_{2,3}$, and R_D are described as

$$\overline{i_{n,o,M_1}{}^2} = \frac{R_{\rm bleed}}{R_{\rm bleed} + R_{\rm sw}} \cdot 4kT\gamma g_{m1} \approx 4kT\gamma g_{m1} \tag{9}$$

$$\overline{i_{n,o,M_4}{}^2} = \frac{r_{o1}}{r_{o1} + R_{\rm sw}} \cdot \frac{1}{(1 + g_{m4}Z_{mm})^2} \cdot 4kT\gamma g_{m4} \approx \frac{1}{(1 + g_{m4}Z_{mm})^2} \cdot 4kT\gamma g_{m4} \tag{10}$$

$$\overline{i_{n,o,M_{2,3}}{}^2} = 8kT\gamma \frac{4I}{ST_{LO}} \tag{11}$$

$$\overline{i_{n,o,R_D}{}^2} = \frac{8kT\gamma}{R_L}. \tag{12}$$

Here, k is the Boltzmann constant; T is the room temperature in kelvins; γ is the channel noise factor; Z_{mm} is the impedance, which is connected to the source of M_4; I is the bias current of switch; S is the slope of the LO signal at the switching instant; $T_{\rm LO}$ is the LO period; and R_L is the load resistor. Generally, the noise from the switch is the dominant noise source. According to (11), the current of the switch is reduced to minimize its noise contribution, but the current of the bleeding path is increased. It can affect the total noise of the mixer, but the increased noise from the nMOS is attenuated by Z_{mm}. This can be explained by the mechanism of source degeneration. The gate-to-source voltage induced by the noise source of M_4 is decreased by source degeneration impedance Z_{mm}. Note that Z_{mm} should be large enough to suppress the noise from the bleeding path, and it is shown as

$$Z_{mm} = j\omega L_m + r_{o1} \left\| \frac{1}{g_{m2,3}} \right\| \frac{1}{j\omega C_p}. \tag{13}$$

From (13), L_m affects the degeneration impedance at high frequency, and the $1/g_{m2,3}$ of the switch affects it at low frequency.

Authorized licensed use limited to: Southern University of Science and Technology. Downloaded on May 28,2024 at 04:56:57 UTC from IEEE Xplore. Restrictions apply.

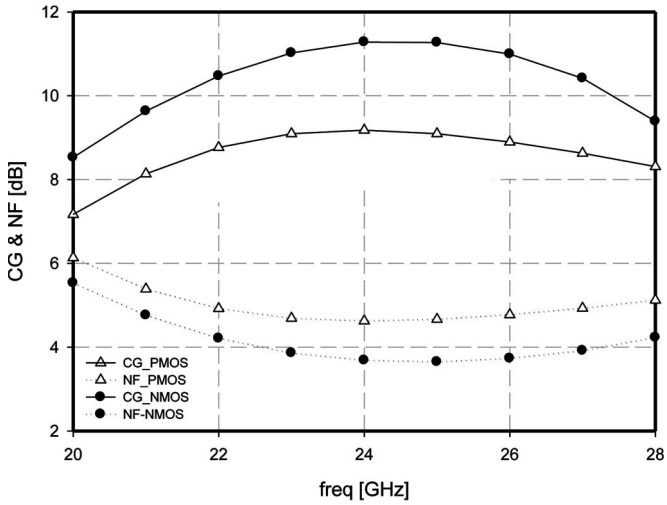

Fig. 3. Comparison of simulated conversion gains and noise figures of nMOS and pMOS bleeding path (IF = 300 MHz).

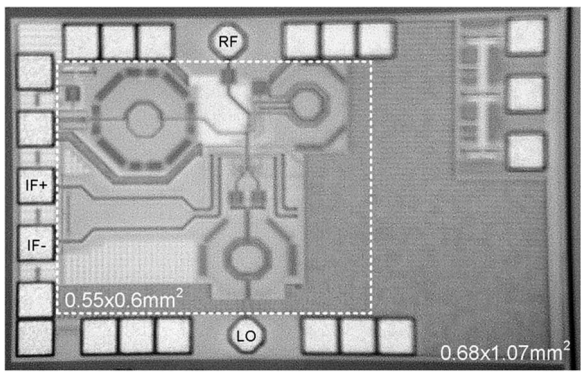

Fig. 4. Microphotograph of the proposed mixer.

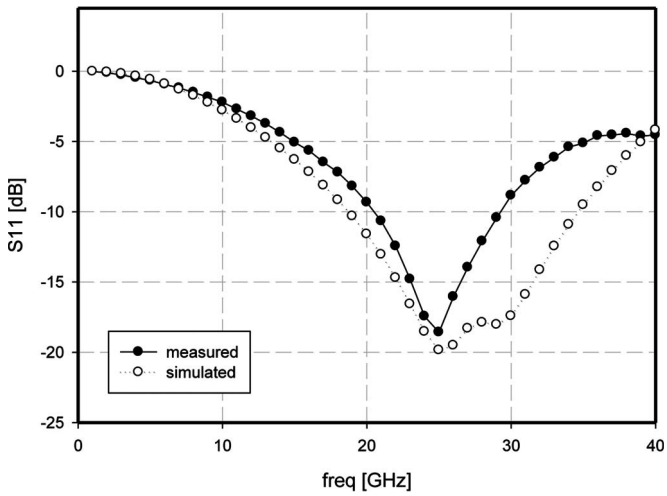

Fig. 5. Measured and simulated S_{11}.

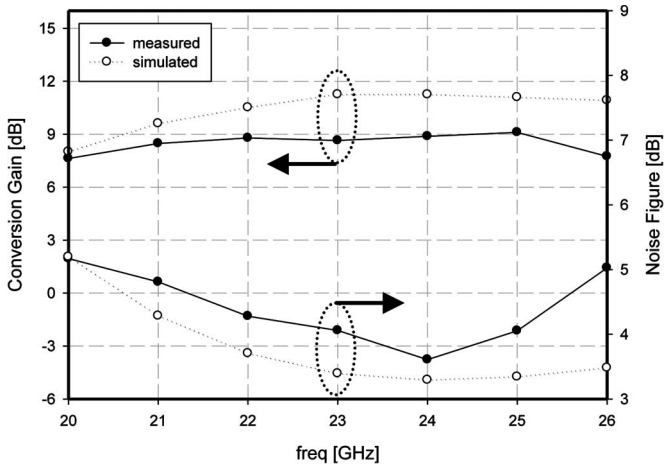

Fig. 6. Measured and simulated conversion gains and noise figures (IF = 300 MHz).

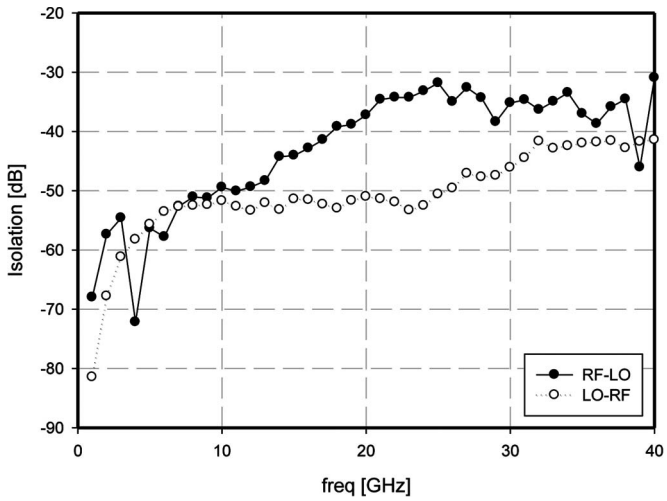

Fig. 7. Measured RF–LO and LO–RF isolations.

Improved noise performance is confirmed by comparing the proposed low-noise mixer with an nMOS bleeding path with the conventional mixer with a pMOS bleeding path. The conventional and proposed mixers have the same size common-gate input stage and the same total power consumption for a fair comparison. The bleeding path of the conventional mixer uses a pMOS current source, and the current ratio of the bleeding path to the switch is set to be equal to that of the proposed one. With the optimum value of the inductor in the conventional mixer, C_p is cancelled out. The total input-referred noises of each mixer are given by (14) and (15), shown at the bottom of the page.

Equation (14) expresses the input-referred noise of the conventional mixer with the pMOS bleeding path, and (15) expresses that of the proposed mixer with the nMOS bleeding

$$\overline{v_{n,\mathrm{in,pMOS\_bleeding}}^2} = \left(4kT\gamma g_{m1} + 4kT\gamma g_{m4} + 4kT\gamma \cdot \frac{4I}{ST} + \frac{4kT}{R_D}\right) \Big/ \frac{4}{\pi^2}(1+nk)^2 {g_{m1}}^2 \tag{14}$$

$$\overline{v_{n,\mathrm{in,nMOS\_bleeding}}^2} = \left(4kT\gamma g_{m1} + \frac{1}{(1+g_{m4}Z_{mm})^2} \cdot 4kT\gamma g_{m4} + 4kT\gamma \cdot \frac{4I}{ST} + \frac{4kT}{R_D}\right) \Big/ \frac{4}{\pi^2}(1+g_{m4}u \cdot Z_m)^2(1+nk)^2 {g_{m1}}^2 \tag{15}$$

Authorized licensed use limited to: Southern University of Science and Technology. Downloaded on May 28,2024 at 04:56:57 UTC from IEEE Xplore. Restrictions apply.

TABLE I
PERFORMANCE SUMMARY OF THE PROPOSED MERGED LNA AND MIXER WITH THE OTHER WORK

Ref.	freq. (GHz)	CG (dB)	NF (dB)	P_{1dB} (dBm)	P_{DC} (mW)	Supply (V)	FoM [b]	technology
[8]	20-32	3	7.5	-	18	1.8	7.7	0.18μm SiGe
[9]	21-24	4.8	10.4	-32	2	1	2.8	0.18μm SiGe
[10]	20-25 [a]	10.5	4.7	-7.2	39	3.3	10.8	0.35μm SiGe
[10]	20-25 [a]	7	7.5	-12	4.2	1.5	13.6	0.13μm CMOS
This work	20-26	9.15	3.61	-13	2.6	1.5	20.1	0.13μm CMOS

[a] graphically estimated. [b] FoM = $10\log((10^{G/20}10^{(IIP3-10)/20})/(10^{NF/10}P))$ [11]. IIP3 is estimated by IIP3 = P_{1dB} + 9.6dB except [8].

path. A comparison of the denominator of (14) and that of (15) confirms that the total noise of the proposed mixer is reduced by a factor of $(1 + g_{m4}u \cdot Z_{\rm mm})^2$ with the increased conversion gain, which is from the boosted transconductance without additional current consumption. The second term of (15), i.e., noise from bleeding path, is decreased by a factor of $(1 + g_{m4}Z_{\rm mm})^2$ by the source degeneration with Z_{mm}. The total noise of the proposed mixer is effectively reduced by the bleeding path g_m-boosting technique. Fig. 3 shows the simulated conversion gains and noise figures of the proposed mixer and the conventional mixer (IF $= 300$ MHz). The conversion gain is increased by approximately 2 dB, and the noise figure is decreased by approximately 1 dB by using the nMOS bleeding path.

The measured and simulated S_{11} is illustrated in Fig. 5. It shows 21–29 GHz wideband input matching. It was measured using an Anritsu 37397D vector network analyzer (VNA). A ground–signal–ground probe was used to apply the RF and LO input signals for all measurements. The IF output signal was measured using an external balun with bond wires.

IV. CHIP IMPLEMENTATION AND MEASUREMENT RESULTS

Fig. 4 shows a microphotograph of the proposed mixer with a whole chip area of 0.68×1.07 mm^2, including bonding pads. It was fabricated in Taiwan Semiconductor Manufacturing Company (TSMC) 0.13-μm one-poly eight-metal CMOS technology. The whole chip consumes a dc power of 23.2 mW at a 1.5-V supply voltage with the IF buffer for 50 Ω matching only for measurement. The circuit without the IF buffer consumes a dc power of 2.6 mW at a 1.5-V supply voltage. The gain of the IF buffer is 0.9 V/V, but the IF buffer consumes high current because of the small $R_{\rm buff}$, which is the load resistor of the buffer. All measurement results are attained with the buffer.

The conversion gain and the noise figure were measured and simulated and are shown in Fig. 6. An Anritsu 37397D VNA was used as an RF source in continuous-wave mode, and an Anritsu MG3694A signal generator was used as an LO frequency source. The downconverted IF signal was measured by an Agilent E4440A spectrum analyzer. The noise figure was measured using an Agilent N8975A noise figure analyzer with an Agilent N4002A smart noise source. The LO power was 0 dBm in the measurements. The IF was 300 MHz when the RF was swept from 20 to 26 GHz, limited by the performance of the equipment, and the lowest noise figure and the highest conversion gain are 3.61 and 9.15 dB, respectively. The measured RF–LO and LO–RF isolations are under -30 and -40 dB in the range of 20–30 GHz, as shown in Fig. 7. The measured $P_{1\ \rm dB}$ is -13 dBm with an RF of 24 GHz, an IF of 300 MHz, and an LO power of 0 dBm.

Table I shows the summarized performance of the proposed low-noise mixer and its comparison with the performance of other state-of-the-art mixers. The proposed circuit has the highest figure of merit (FoM) with the lowest noise figure [11].

V. CONCLUSION

A K-band UWB CMOS low-noise mixer has been implemented. It has low power consumption, a wide bandwidth, and a low noise figure. The noise sources of the mixer are reduced by the proposed bleeding path g_m-boosting technique. These allow the minimum noise figure of 3.61 dB while consuming the dc power of 2.6 mW at a 1.5-V supply. The measurement results show a conversion gain of 9.15 dB, a $P_{1\ \rm dB}$ of -13 dBm, and an RF bandwidth of 20–26 GHz. The circuit was fabricated in TSMC 0.13-μm one-poly eight-metal CMOS technology with a chip area of 0.68×1.07 mm^2.

REFERENCES

[1] "Technical requirements for vehicular radar systems," FCC, Washington, DC, USA, FCC 47 CFR, Sec. 15.515, 2008.

[2] B. Razavi, *RF Microelectronics*. Englewood Cliffs, NJ, USA: Prentice-Hall, 1998.

[3] M. A. Richards, *Fundamentals of Radar Signal Processing*. New York, NY, USA: McGraw-Hill, 2005.

[4] X. Li, S. Shekhar, and D. J. Allstot, " G_m-boosted common-gate LNA and differential Colpitts VCO/QVCO in 0.18- μm CMOS," *IEEE J. Solid-State Circuits*, vol. 40, no. 12, pp. 2609–2619, Dec. 2005.

[5] Z. Zhang, Z. Chen, and J. Lau, "A 900 MHz CMOS balanced harmonic mixer for direct conversion receivers," in *Proc. IEEE Radio Wireless Conf.*, Sep. 2000, pp. 219–222.

[6] J. Park, C. H. Lee, B. S. Kim, and J. Laskar, "Design and analysis of low flicker-noise CMOS mixers for direct-conversion receivers," *IEEE Trans. Microw. Theory Tech.*, vol. 54, no. 12, pp. 4372–4380, Dec. 2006.

[7] H. Darabi and A. A. Abidi, "Noise in RF-CMOS mixers: A simple physical model," *IEEE J. Solid-State Circuits*, vol. 35, no. 1, pp. 15–25, Jan. 2000.

[8] M. El-Nozahi, E. Sánchez-Sinencio, and K. Entesari, "A 20–32 GHz wideband mixer with 12 GHz IF bandwidth in 0.18- μm SiGe process," *IEEE Trans. Microw. Theory Tech.*, vol. 58, no. 11, pp. 2731–2740, Nov. 2010.

[9] N. Shiramizu, T. Masuda, T. Nakamura, and K. Washio, "24-GHz 1-V pseudo-stacked mixer with gain-boosting technique," in *Proc. ESSCIRC*, Sep. 2008, pp. 102–105.

[10] V. Issakov, H. Knapp, M. Tiebout, A. Thiede, W. Simburger, and L. Maurer, "Comparison of 24 GHz low-noise mixers in CMOS and SiGe: C technologies," in *Proc. EuMIC*, 2009, pp. 184–187.

[11] V. Vidojkovic, J. van der Tang, A. Leeuwenburgh, and A. H. M. V. Roermund, "A low-voltage folded-switching mixer in 0.18 μm CMOS," *IEEE J. Solid-State Circuits*, vol. 40, no. 6, pp. 1259–1264, Jun. 2005.

Authorized licensed use limited to: Southern University of Science and Technology. Downloaded on May 28,2024 at 04:56:57 UTC from IEEE Xplore. Restrictions apply.